3D-reconstruction of gamma-ray showers with a stereoscopic system

M. Lemoine-Goumard

3D-reconstruction of gamma-ray showers with a stereoscopic system

Marianne Lemoine-Goumard for the H.E.S.S. Collaboration

Laboratoire Leprince-Ringuet
École Polytechnique - CNRS/IN2P3
F-91128 Palaiseau Cedex, France

We report on a new 3D-reconstruction of γ-ray showers which takes full advantage of the assets of a stereoscopic system of atmospheric Cherenkov telescopes and of the fine-grain imaging. The rich information collected by the cameras allows us to discriminate γ-ray showers and hadronic showers on the basis of two simple properties of electromagnetic showers : their rotational symmetry with respect to the axis and their relatively small lateral spread. The performance of the method is presented in terms of γ-ray efficiency, angular resolution and spectral resolution.

1 Introduction

The method described here is based on a simple 3D-modeling of the light emitted by an electromagnetic air shower. The rich information contained in several fine-grained images of such a shower provides enough constraints to allow an accurate reconstruction, even by means of a simple model essentially based on the rotational symmetry of the electromagnetic cascade with respect to its incident direction. This allows to select γ-ray induced showers on the basis of only two criteria with a direct physical meaning : rotational symmetry and small lateral spread. This method provides an efficient rejection of hadronic showers even without using the shower direction (particularly important for the study of extended sources such as Supernova Remnants), while keeping a γ-ray efficiency as high as 80%. Comparison of this method with other ones applied in the H.E.S.S. experiment can be found in reference [1].

2 The reconstruction method

2.1 Modeling assumptions

The most important characteristics of electromagnetic showers is that the spatial distribution of the emission points of Cherenkov photons and the angular distribution of these photons with respect to the shower axis, are on average rotationally symmetric with respect to the shower axis. The 3D-model of γ-ray showers presented here is based on two simplifying assumptions :

- The emission points of Cherenkov photons are distributed according to a 3-dimensional Gaussian law with rotational symmetry with respect to the shower axis; it is thus characterized by the following parameters : the direction of the shower in the reference frame of the telescope, the position of the core on the ground, the altitude of shower maximum, the longitudinal (σ_L) and transverse (σ_T) standard deviations of the Gaussian distributions, referred to as "3D-length" and "3D-width" respectively, and the total number N_c of Cherenkov photons emitted by the shower. The preceding quantities, referred to as "shower parameters", will be determined by a maximum likelihood fit.

- The same anistropic angular distribution of Cherenkov photons with respect to the shower axis has been assumed for all emission points and for all shower energies.

2.2 Implementation of the method

The preceding 3D-model enables us to work out the expected number of Cherenkov photons q_{th} collected by a given pixel of a given telescope as a function of the shower parameters listed above by an integration along the line of sight of each pixel. The quantities q_{th} for all pixels, calculated for a set of shower parameters, are further used to build up a likelihood function for each event including at least two images for a given shower. The likelihood function for each event is then maximized with respect to the 8 shower parameters defined above.

3 Gamma-ray selection based on shower shape

3.1 Longitudinal development: physical condition for γ-rays

Since only one length scale, namely the radiation length, governs the development of electromagnetic showers both longitudinally and laterally, it is convenient to express characteristic lengths in units of radiation lengths (or equivalently in "air thickness"
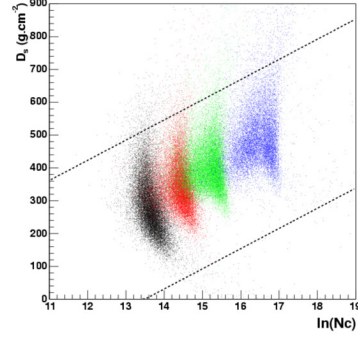
Figure 1: *Simulated γ-ray showers: depth of shower maximum D_s as a function of the logarithm of the total number N_c of Cherenkov photons, for different values of the primary energy E_0 (from left to right: 200 GeV, 500 GeV, 1 TeV, 5 TeV) at zenith.*
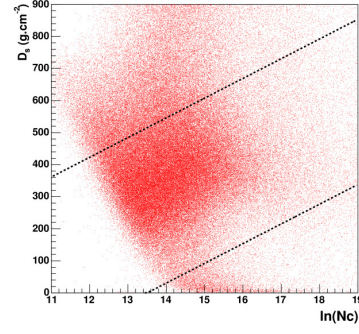

Figure 2: *Showers from a field of view free of γ-ray source reconstructed as if they were electromagnetic showers: depth of shower maximum D_s as a function of the logarithm of the total number N_c of Cherenkov photons. The observation was performed at a zenith angle of $16°$.*

in g cm^{-2}). In γ-ray showers, the slant depth of shower maximum (obtained from the likelihood fit), is correlated to the primary energy, thus to the total number of Cherenkov photons Nc, as shown by simulations (figure 1). On the other hand, the fit, as applied to hadron showers, sometimes converges towards very small or, more often towards very large depths (figure 2). Thus we can define another constraint characterizing γ-rays : the fitted parameters D_s (in g cm^{-2}) and N_c are required to satisfy the following condition :

$$61.5 \left(\ln N_c - 13.5 + T(\zeta) \right) \leq D_s \ \leq 61.5 \left(\ln N_c - 10 + T(\zeta) \right) + 300 \quad (1)$$

with $T(\zeta) = 3.28(1 - \cos \zeta)$, this last term being introduced since the relation between the reconstructed value of N_c and the estimated value of the primary energy depends on ζ. Events satisfying condition (1) are represented in the region between the two straight lines shown in figure 1 for showers at zenith.

3.2 Lateral development of the shower

The potentiality of the 3D-width σ_T for discriminating γ-rays from hadrons is illustrated in figure 3, obtained from the analysis of H.E.S.S. data (4 hours live time) taken
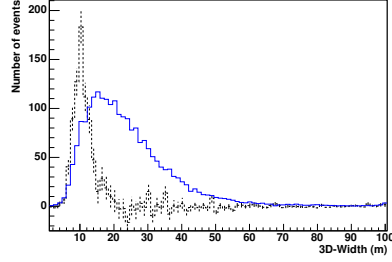
Figure 3: *Distribution of σ_T for γ-rays (dotted line) obtained from real data taken on PKS2155 by subtracting the background from on-source data; the background distribution is given by the solid line.*
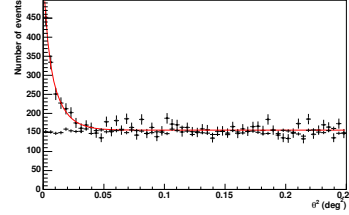

Figure 4: *θ^2 distribution.from data taken on PKS2155-304 in 2004: (a) Filled circles: "on source" region. (b) Crosses: background control regions.(c) The curve is the fitted point-spread function.*

in 2004 on the blazar PKS2155-304 with a mean zenith angle of $30°$ and an offset angle of $0.5°$. The background contribution was obtained from 5 off-source regions with the same acceptance as the source region. As one can see on this figure, the hadronic showers which fit the model are generally much broader than electromagnetic ones, due to the higher transverse momenta of secondary particles in strong interactions.

It is also convenient to express σ_T in "air thickness" in g cm^{-2}, i.e. to use the quantity $\sigma'_T = \sigma_T \, \rho(z_{max})$, in which $\rho(z_{max})$ is the density of air at the altitude z_{max} of the barycentre. For simulated γ-ray showers of different primary energies, the depth of shower maximum D_s is plotted versus σ'_T in figure 5, both quantities being reconstructed by the fit and expressed in g cm^{-2}. Simulations show that, on average, σ'_T scales with D_s (figure 5); this property results from the variation of the Cherenkov threshold with D_s. Consequently, the dimensionless ratio $\omega = \sigma'_T/D_s$ follows a distribution which, in the absence of reconstruction errors, would be independent of the γ-ray energy and zenith angle. In the following, the quantity ω will be referred to as the "reduced 3D-width". Figure 6 shows the σ_T distributions for 1 TeV γ-ray showers at zenith angles $0°$, $46°$ and $60°$; in contrast, figure 7 shows the corresponding distributions for the reduced 3D-width ω, almost identical and concentrated in the region $\omega < 0.002$; only a small extension towards higher values appears at large zenith angles.
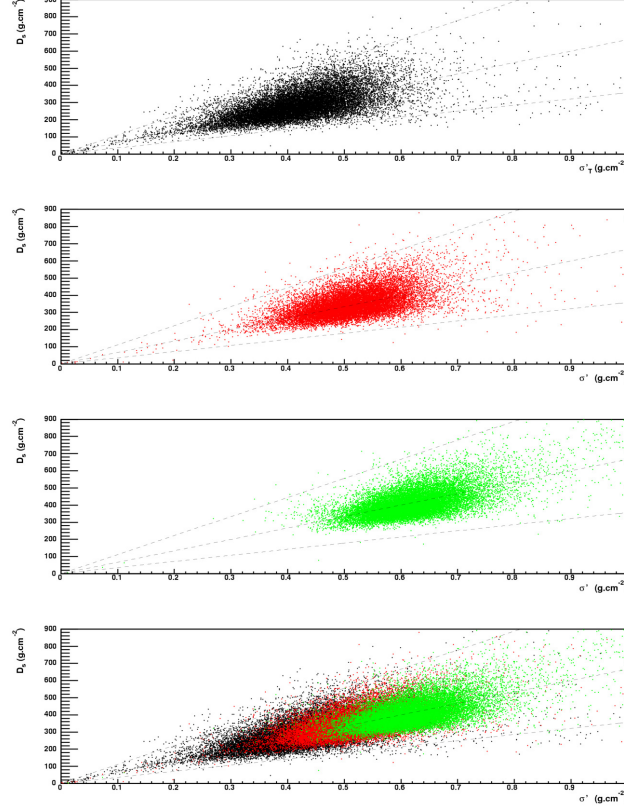
Figure 5: *Simulated γ-ray showers: depth of shower maximum D_s as a function of the 3D-width σ'_T (both reconstructed by the fit and expressed in g cm^{-2}), for different values of the primary energy E_0: from top to bottom, 200 GeV, 500 GeV, 1 TeV, the last plot is the superposition of the preceding ones. The straight lines are intended to guide the eye.*

4 Performance of the method

4.1 Gamma-ray selection efficiency

The similarity between the distributions of ω at different zenith angles and energies allows to select γ-rays by using the same criterium $\omega < 2 \times 10^{-3}$ for all conditions of observation. On the basis of γ-ray simulations at different zenith angles and energies,
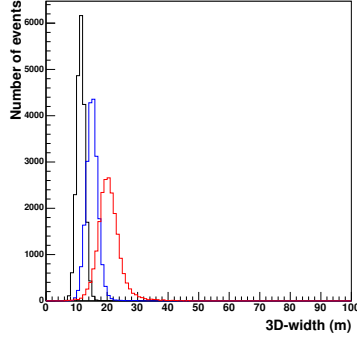
Figure 6: *3D width distributions for 1 TeV γ-ray showers at zenith angles $0°$, $46°$ and $60°$ (from left to right).*
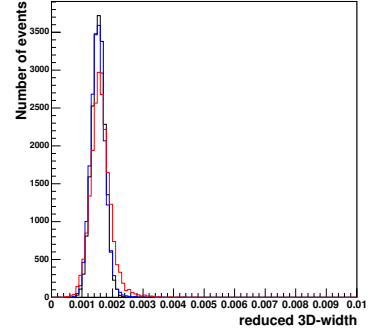

Figure 7: *Distributions of the reduced 3D-width at zenith angles $0°$, $46°$ and $60°$ for 1 TeV γ-ray showers.*
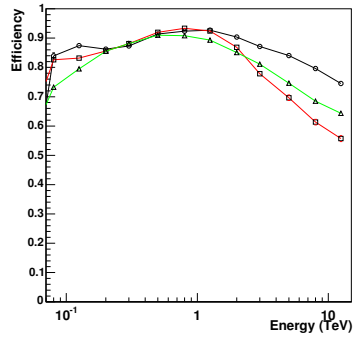

Figure 8: *Reconstruction efficiency for γ-rays at zenith, as a function of the primary energy, for showers viewed by 2 telescopes (triangles), 3 telescopes (squares) and 4 telescopes (circles) respectively.*
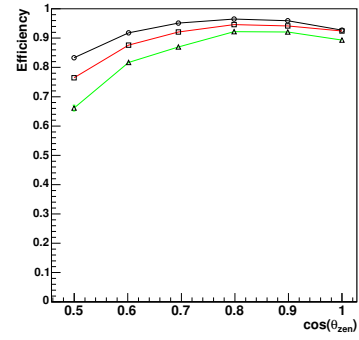

Figure 9: *Reconstruction efficiency for 1 TeV γ-rays on axis as a function of the zenith angle, for showers viewed by 2 telescopes (triangles), 3 telescopes (squares) and 4 telescopes (circles) respectively.*

the selection efficiency ε_s for γ-rays is defined as the fraction of events accepted by the fit and satisfying both the physical condition (1) and $\omega < 2 \times 10^{-3}$. At this level, the selection is only based on the shower shape, not on its direction, as is relevant in the study of extended sources. Figure 8 shows the variation of ε_s at zenith as a function of the primary energy for showers viewed by 2, 3 and 4 telescopes. Similarly, the variation of ε_s as a function of the zenith angle is shown in figure 9 for 1 TeV γ-rays; The relatively high value of ε_s ($> 80\%$ between 100 GeV and 3 TeV at zenith) and its smooth variation over a large range of energies and zenith angles are particularly well suited to spectral analysis.

4.2   Angular resolution

The angular resolution is characterized by the "point-spread function" (PSF), i.e. the distribution of the angle θ between the reconstructed direction and that of the source. Figure 4 shows the θ^2 distribution obtained from the H.E.S.S. data (4 hours live time) taken in 2004 on the blazar PKS2155-304. The PSF is obtained after background subtraction. It is well fitted by a linear superposition of two exponential laws in θ^2; the narrower one characterized by σ_1, is thus superimposed to a broader halo. Figure 10, also obtained from simulations, shows the variation of the spread of the central spot σ_1 as a function of the γ-ray energy for different zenith angles and on-axis showers; all events viewed by 2, 3 or 4 telescopes are included. This spread is practically always smaller than $0.06°$ (about $4'$) and remains fairly constant at energies greater than 1 TeV. In order to take the halo into account, one can also characterize the angular distribution by the angular radius R_{68} of the cone centered on the true γ-ray direction and containing 68% of the reconstructed axes. Its variation as a function of the γ-ray energy for different zenith angles is shown in figure 11.

5   Energy resolution

The energy E_0 of the primary γ-ray is reconstructed calorimetrically from the total number of Cherenkov photons N_c obtained from the fit. If the 3D-model of the shower described above were a perfect representation of the electromagnetic shower, N_c would be, on average, almost[1] proportional to E_0. As a matter of fact, simulations of γ-ray showers for fixed values of E_0, show that the average value of $\ln N_c$ (noted as $< \ln N_c >$), obtained from the likelihood fit, varies almost linearly with $\ln E_0$ for fixed observing conditions, namely: number of telescopes viewing the shower n_T, direction of the telescope axes (i.e. zenith angle ζ), direction of the shower axis (i.e.

---

[1]The variation of the Cherenkov threshold as a function of the altitude makes this statement only approximative.
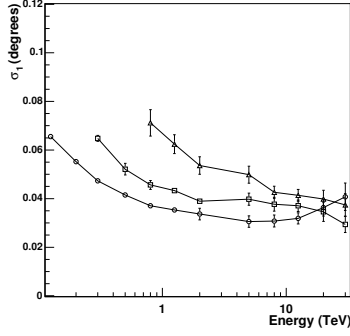
Figure 10: *Central spot spread σ_1, as a function of γ-ray energy for zenith angles 0° (circles), 46° (squares) and 60° (triangles).*
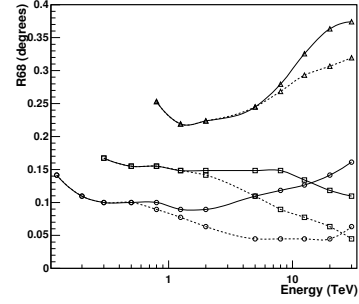

Figure 11: *Radius of the 68% confidence level region, as a function of γ-ray energy for zenith angles 0° (circles), 46° (squares) and 60° (triangles). Dotted lines show the effect of an additional cutoff requiring at least two images whose centre of gravity is within 2° from the camera centre.*

offset angle α). However, as an effect of the approximations of the 3D-model used in the fit, the coefficients a and b in the formula $< \ln N_c > = a \ln E_0 + b$ depend on the observing conditions. Therefore, the estimator is based essentially on the value of N_c, but also on n_T, ζ, α and distance of the shower core d_T. Simulations for fixed values of these parameters provide a relation between $< \ln N_c >$ and $\ln E_0$ which can be generalized to arbitrary values of ζ, α and d_T through interpolations. This same relation is then used for a given event satisfying the likelihood fit to find the energy estimator E_r as a function of N_c, n_T, ζ, α and d_T. The distribution of $\ln(E_r/E_0)$ is found to be Gaussian to a good approximation for all observing conditions. These Gaussian distributions are characterized by their bias $\delta = < \ln(E_r/E_0) >$ and their standard deviation $\sigma(\ln(E_r/E_0)) \approx \Delta E_r/E_r$. The variations of δ and of $\Delta E_r/E_r$ with energy at different zenith angles are shown in figure 12.

6 Conclusion

The reconstruction method described above is conceptually simple and has been succesfully applied to H.E.S.S. data. With a minimal set of cuts, the selection efficiency
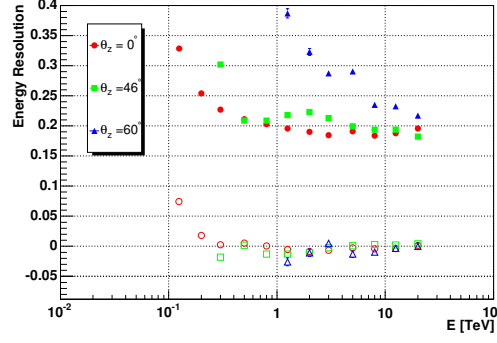
3D-reconstruction of gamma-ray showers with a stereoscopic system
Marianne Lemoine-Goumard et al.

Figure 12: *Energy measurement at different zenith angles ζ. Open symbols: bias δ in $\ln(E_r/E_0)$ as a function of the true primary energy E_0; filled symbols: standard deviation of $\ln(E_r/E_0)$ as a function of E_0. Circles are for $\zeta = 0°$, squares for $\zeta = 46°$ and triangles for $\zeta = 60°$.*

is rather uniform between 10 GeV and 10 TeV and of the order of 80%. In addition, the distribution of the "reduced 3D-width" ω, is found to be almost independent of the γ-ray energy and zenith angle and γ-rays can be efficiently selected by requiring $\omega < 2 \times 10^{-3}$ for all observing conditions. This criterium provides a γ-ray/hadron discrimination completely independent of simulations.

References

[1] M. de Naurois, "Analysis methods for IACTs", *these proceedings pp. 149-161*